ARTICLE

Electronic supplementary information (ESI) for the article:

Solution and solid state studies of hydrogen bonding in substituted oxazolidinones by spectroscopic and quantum chemical methods

Received 00th January 20xx,
Accepted 00th January 20xx

DOI: 10.1039/x0xx00000x

To be published in:
New Journal of Chemistry

Tomislav Jednačak,*[a] Maja Majerić Elenkov,[b] Tomica Hrenar,[a] Karlo Sović,*[a] Jelena Parlov Vuković[c] and Predrag Novak[a]

[a.] *Department of Chemistry, Faculty of Science, University of Zagreb, Horvatovac 102a, HR-10000 Zagreb, Croatia. E-mails: tjednacak@chem.pmf.hr; karlo.sovic@chem.pmf.hr*; Tel: +385 1 460 61 95; +385 1 460 60 09
[b.] *Ruđer Bošković Institute, Bijenička cesta 54, HR-10000, Zagreb, Croatia*
[c.] *Central testing laboratory, Refining & marketing business division, INA-Industrija nafte d.d., Lovinčićeva 4, HR-10000 Zagreb, Croatia*

Table S1 Proton chemical shifts of **1b** and **1c** in DMSO-d_6, $CDCl_3$ and CD_3OD at room temperature

Atom	$\delta(^1H)$/ppm					
	1b			**1c**		
	DMSO-d_6	$CDCl_3$	CD_3OD	DMSO-d_6	$CDCl_3$	CD_3OD
3	7.61	5.82	4.59	7.40	5.82	4.60
4	3.21, 3.59	3.51, 3.77	3.45, 3.74	3.08, 3.52	3.25, 3.67	3.23, 3.66
5	4.81	4.85	4.91	4.46	4.58	4.60
6	3.69, 3.75	3.52, 3.58	3.65, 3.71	1.59, 1.62	1.71, 1.81	1.71, 1.74
6-Me	–	–	–	0.89	1.01	1.00

Table S2 Proton chemical shifts of **2b** and **2c** in DMSO-d_6, $CDCl_3$ and CD_3OD at room temperature

Atom	$\delta(^1H)$/ppm					
	2b			**2c**		
	DMSO-d_6	$CDCl_3$	CD_3OD	DMSO-d_6	$CDCl_3$	CD_3OD
3	7.60	5.85	4.88	7.38	5.91	4.58
4	3.27, 3.41	3.38, 3.71	3.66	3.14, 3.25	3.27, 3.40	3.28, 3.41
5-Me	1.47	1.66	1.60	1.30	1.44	1.41
6	3.72	3.47, 3.58	3.64, 3.69	1.60, 1.63	1.72, 1.76	1.71, 1.75
6-Me	–	–	–	0.87	0.98	0.97

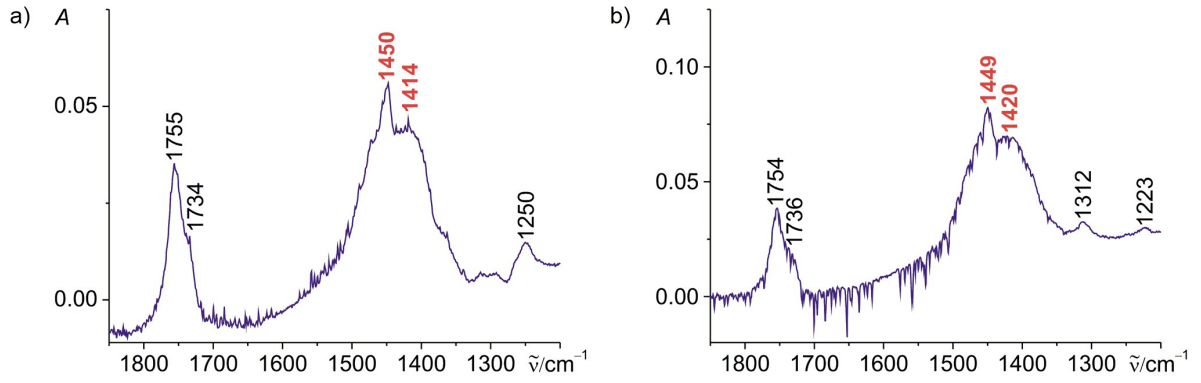

Fig. S1 ATR-IR spectra of (a) **1a** and (b) **2a** in CH_3OH in the range 1850–1200 cm^{-1}. Wavenumbers corresponding to the solvent vibrational bands are shown in bold and red.

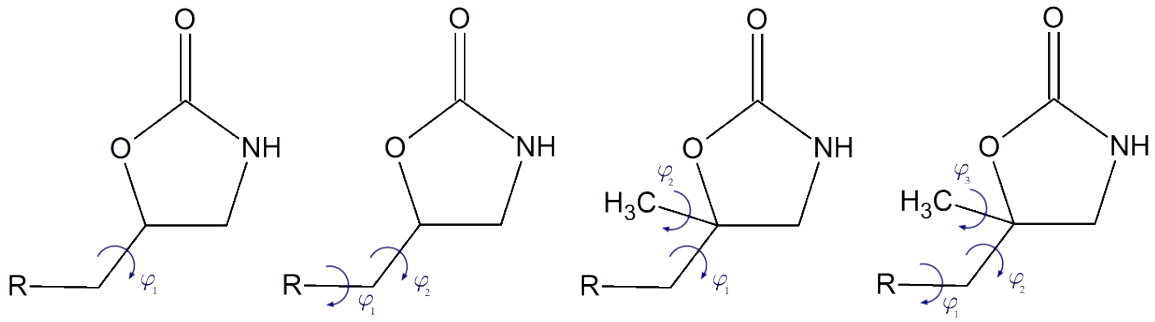

1a: R = Cl
1b: R = Br

1c: R = Me

2a: R = Cl
2b: R = Br

2c: R = Me

Scheme S1 Relevant torsional coordinates for compounds **1a–1c** and **2a–2c**.

Table S3 Calculated standard Gibbs energies of formation and content at T = 298.15 K and p = 101325 Pa for conformers of **1a** (B3LYP/6-311++g(d,p) level of theory, relative to the most stable conformer)

Conformer	$\Delta_f G°_{rel.}$ / kcal mol^{-1}	Content / %
1a1	0.00	84.3
1a2	1.13	12.4
1a3	1.92	3.3

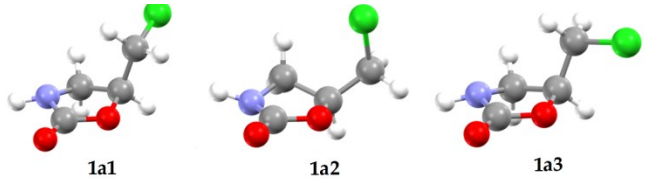

Fig. S2 Conformers of **1a** (B3LYP/6-311++g(d,p) level of theory).

Table S4 Calculated standard Gibbs energies of formation and content at T = 298.15 K and p = 101325 Pa for conformers of **2a** (B3LYP/6-311++g(d,p) level of theory, relative to the most stable conformer)

Conformer	$\Delta_f G°_{rel.}$ / kcal mol^{-1}	Content / %
2a1	0.00	87.4
2a2	1.29	9.85
2a3	2.05	2.75

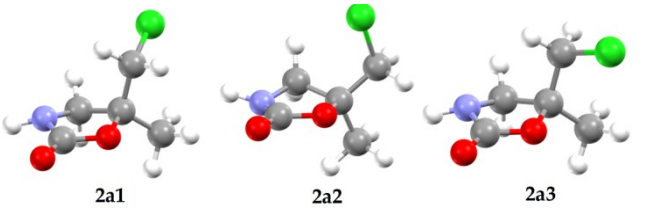

Fig. S3 Conformers of **2a** (B3LYP/6-311++g(d,p) level of theory).

Table S5 Calculated standard Gibbs energies of formation and content at T = 298.15 K and p = 101325 Pa for conformers of **1b** (B3LYP/6-311++g(d,p) level of theory, relative to the most stable conformer)

Conformer	$\Delta_f G°_{rel.}$ / kcal mol^{-1}	Content / %
1b1	0.00	78.1
1b2	0.79	20.6
1b3	2.42	1.3

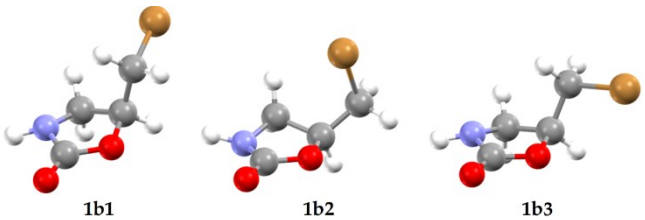

Fig. S4 Conformers of **1b** (B3LYP/6-311++g(d,p) level of theory).

Table S6 Calculated standard Gibbs energies of formation and content at T = 298.15 K and p = 101325 Pa for conformers of **2b** (B3LYP/6-311++g(d,p) level of theory, relative to the most stable conformer)

Conformer	$\Delta_f G°_{rel.}$ / kcal mol^{-1}	Content / %
2b1	0.00	86.3
2b2	1.16	12.2
2b3	2.40	1.5

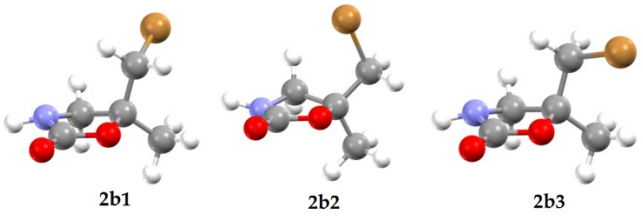

Fig. S5 Conformers of **2b** (B3LYP/6-311++g(d,p) level of theory).

Table S7 Calculated standard Gibbs energies of formation and content at T = 298.15 K and p = 101325 Pa for conformers of **1c** (B3LYP/6-311++g(d,p) level of theory, relative to the most stable conformer).

Conformer	$\Delta_f G°_{rel.}$ / kcal mol^{-1}	Content / %
1c1	0.00	60.9
1c2	0.47	27.7
1c3	0.99	11.4

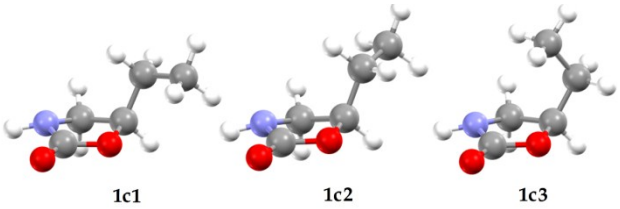

Fig. S6 Conformers of **1c** (B3LYP/6-311++g(d,p) level of theory).

Table S8 Calculated standard Gibbs energies of formation and content at T = 298.15 K and p = 101325 Pa for conformers of **2c** (B3LYP/6-311++g(d,p) level of theory, relative to the most stable conformer)

Conformer	$\Delta_f G°_{rel.}$ / kcal mol^{-1}	Content / %
2c1	0.00	40.5
2c2	0.01	39.7
2c3	0.42	19.8

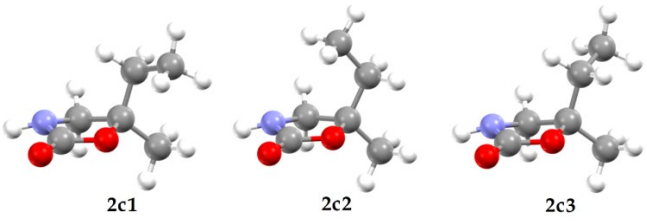

Fig. S7 Conformers of **2c** (B3LYP/6-311++g(d,p) level of theory).

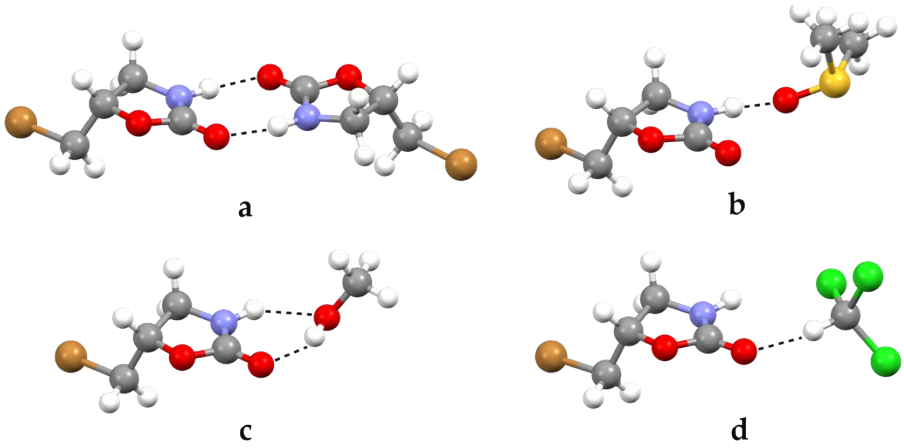

Fig. S8 Optimised geometries of (a) **1b** dimer, (b) **1b**–DMSO complex, (c) **1b**–MeOH complex and (d) **1b**–$CHCl_3$ complex at the B3LYP/6-311++G(d,p) level of theory using IEFPCM for incorporating solvent effects.

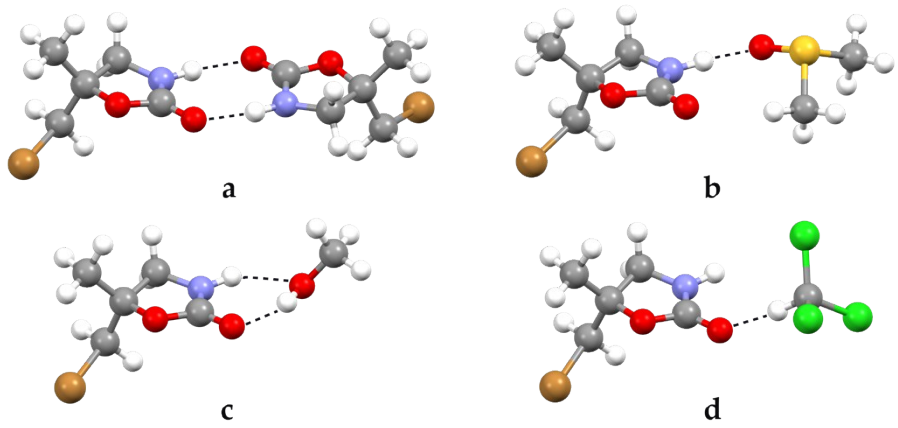

Fig. S9 Optimised geometries of (a) **2b** dimer, (b) **2b**–DMSO complex, (c) **2b**–MeOH complex and (d) **2b**–$CHCl_3$ complex at the B3LYP/6-311++G(d,p) level of theory using IEFPCM for incorporating solvent effects.

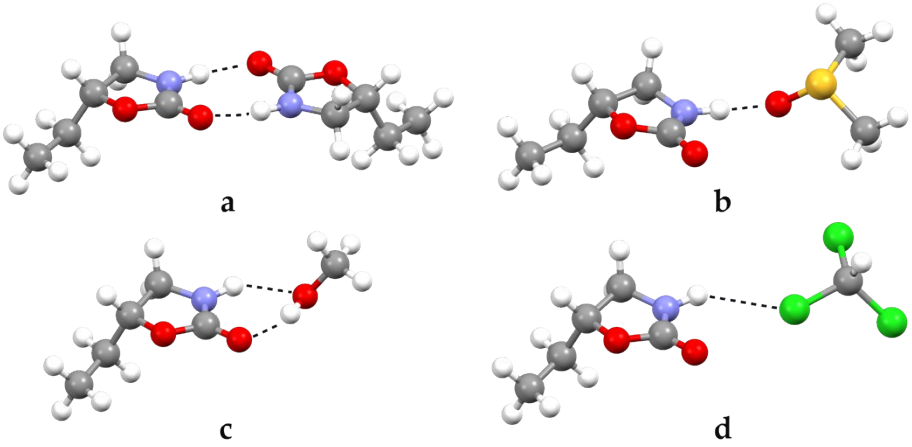

Fig. S10 Optimised geometries of (a) **1c** dimer, (b) **1c**–DMSO complex, (c) **1c**–MeOH complex and (d) **1c**–$CHCl_3$ complex at the B3LYP/6-311++G(d,p) level of theory using IEFPCM for incorporating solvent effects.

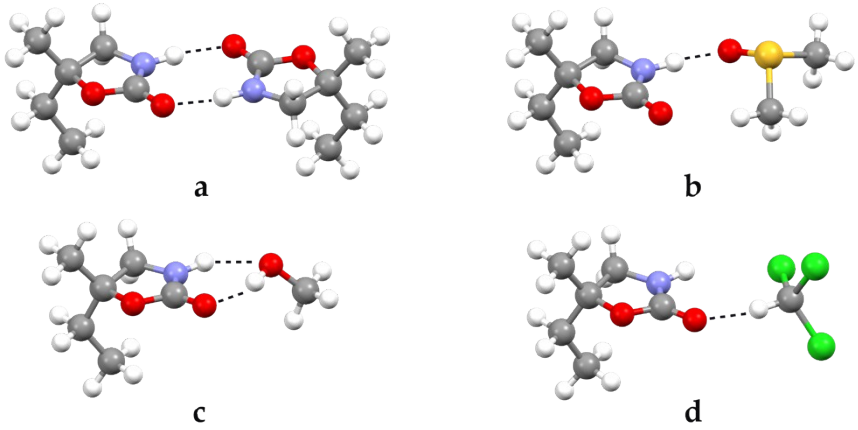

Fig. S11 Optimised geometries of (a) **2c** dimer, (b) **2c**–DMSO complex, (c) **2c**–MeOH complex and (d) **2c**–$CHCl_3$ complex at the B3LYP/6-311++G(d,p) level of theory using IEFPCM for incorporating solvent effects.

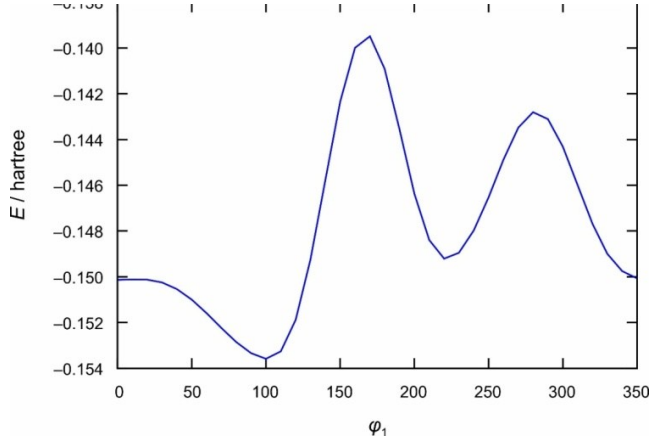

Fig. S12 Potential energy surface of **1a** spanned by one torsional coordinate.

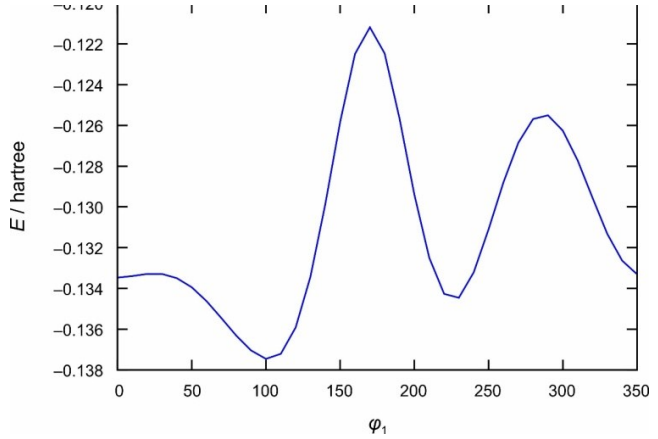

Fig. S13 Potential energy surface of **1b** spanned by one torsional coordinate.

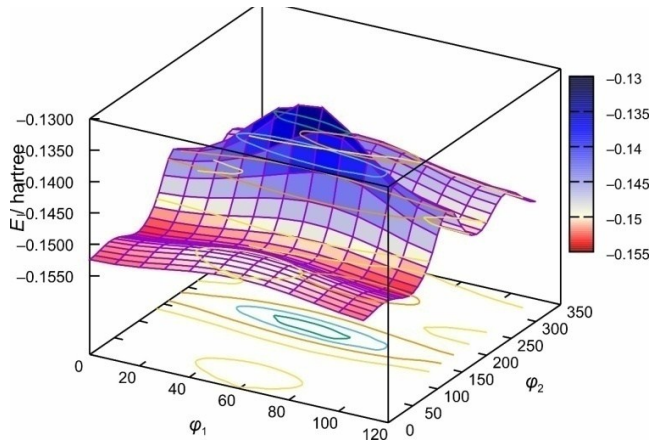

Fig. S14 Potential energy surface of **1c** spanned by two torsional coordinates.

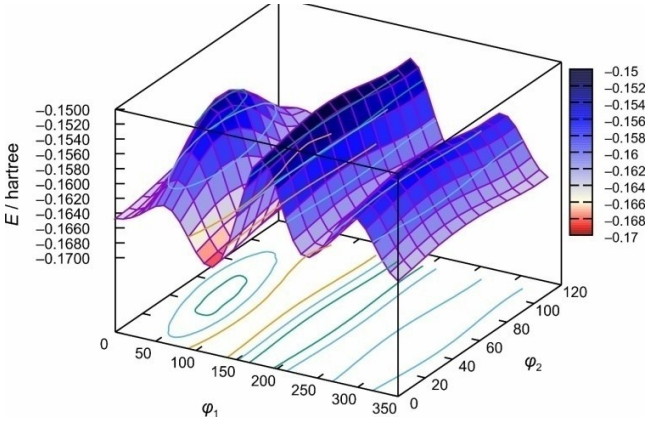

Fig. S15 Potential energy surface of **2a** spanned by two torsional coordinates.

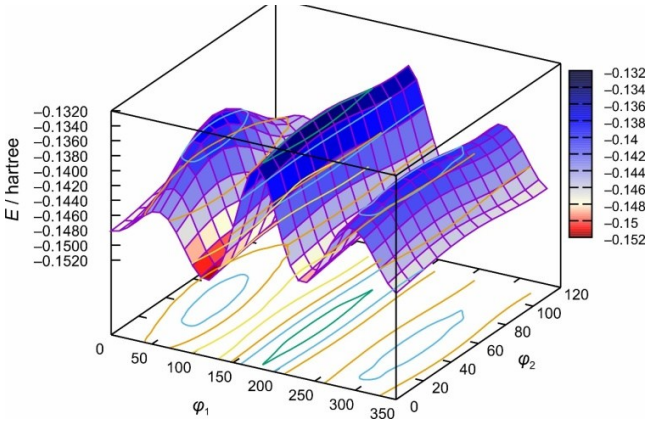

Fig. S16 Potential energy surface of **2b** spanned by two torsional coordinates.

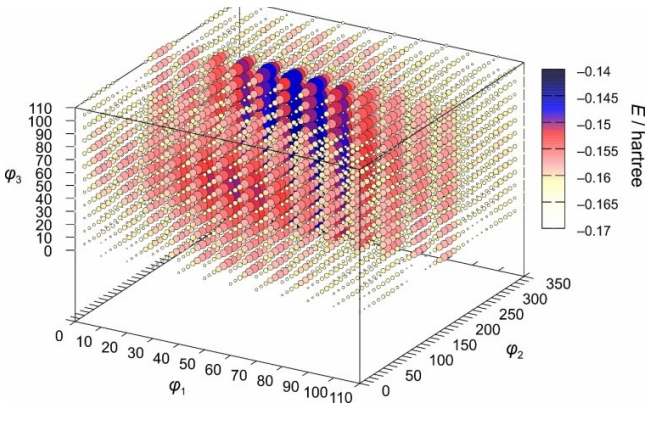

Fig. S17 Potential energy surface of **2c** spanned by three torsional coordinates.

Table S9 Estimation of stability of **1b** complexes by subtraction of standard Gibbs energies of complexes from individual moieties and ordered relative to the most stable configuration (B3LYP/6-311++G(d,p) level of theory and IEFPCM for incorporating solvent effects)

System	IEFPCM solvent	$\Delta\Delta_f G°_{rel.}$ / kJ mol^{-1}
1b–DMSO	dimethylsulfoxide	0.00
1b–**1b**	methanol	11.65
1b–**1b**	dimethylsulfoxide	12.07
1b–**1b**	chloroform	12.15
1b–MeOH	methanol	20.22
1b–$CHCl_3$	chloroform	22.05

Table S10 Estimation of stability of **1c** complexes by subtraction of standard Gibbs energies of complexes from individual moieties and ordered relative to the most stable configuration (B3LYP/6-311++G(d,p) level of theory and IEFPCM for incorporating solvent effects)

System	IEFPCM solvent	$\Delta\Delta_f G°_{rel.}$ / kJ mol^{-1}
1c–**1c**	chloroform	0.00
1c–**1c**	methanol	6.24
1c–**1c**	dimethylsulfoxide	6.55
1c–DMSO	dimethylsulfoxide	7.78
1c–MeOH	methanol	15.81
1c–$CHCl_3$	chloroform	21.77

Table S11 Estimation of stability of **2c** complexes by subtraction of standard Gibbs energies of complexes from individual moieties and ordered relative to the most stable configuration (B3LYP/6-311++G(d,p) level of theory and IEFPCM for incorporating solvent effects).

System	IEFPCM solvent	$\Delta\Delta_f G°_{rel.}$ / kJ mol^{-1}
2c–**2c**	chloroform	0.00
2c–**2c**	methanol	9.26
2c–**2c**	dimethylsulfoxide	9.46
2c–DMSO	dimethylsulfoxide	13.72
2c–MeOH	methanol	15.74
2c–$CHCl_3$	chloroform	17.88

Table S12 Characteristic Raman vibrational modes of **1a**–**1c** and **2a**–**2c**.

Vibrational mode	$\tilde{\nu}$/ cm^{-1}					
	1a	**1b**	**1c**	**2a**	**2b**	**2c**
νC–H)	2966, 2910	2961, 2904	2969, 2912	2961, 2936	2956, 2929	2940, 2905
ν(C=O)	1725	1722	1746, 1706	1719, 1703	1746, 1700	1747, 1698
δ(CH_2)	1493, 1428	1490, 1423	1486, 1436	1487, 1450	1484, 1447	1496, 1452
ν_s(C–O)[a]	1075	1064	1077	1073	1088	1051
ν(C–C)	967	964	988	996	996	988
ν(C–Cl)	735, 656	–	–	750, 705	–	–
ν(C–Br)	–	653, 532	–	–	689, 586	–

[a]ν_s - Symmetric stretching.